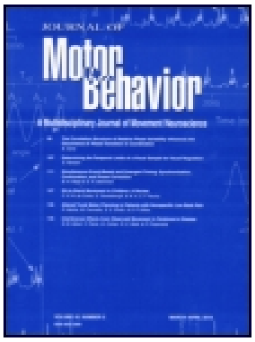

Journal of Motor Behavior

ISSN: 0022-2895 (Print) 1940-1027 (Online) Journal homepage: http://www.tandfonline.com/loi/vjmb20

Dynamics of Pushing

Denis Rancourt & Neville Hogan

Journal of Motor Behavior, 2001, Vol. 33, No. 4, 351–362

Dynamics of Pushing

Denis Rancourt
Neville Hogan
Laval University
Sainte-Foy, Québec
Massachusetts Institute of Technology
Cambridge, MA

ABSTRACT. A standing individual can use several strategies for modulating pushing force magnitude. Using a static model, researchers have shown that the efficacy of those strategies varies considerably. In the present article, the authors propose a human motor control dynamic model for analyzing transients that occur when an individual is asked to modulate force magnitude. According to the model, the impedances of both the upper and the lower limbs influence the time course of force variations and foot placement has a profound effect on pushing force dynamics. With a feet-together posture, the center of pressure has a limited range of motion and changes in force may be preceded by initial changes in the opposite direction; that is, to decrease force, an individual must first increase force. When the feet are placed apart, individuals can move the center of pressure over a much larger range, thereby modulating pushing force magnitude, without reversing behavior, over a larger range of force magnitudes. Therefore, the best way to control pushing force at the hand may be by using the foot.

Key words: equilibrium-point hypothesis, foot placement, force control, hand stiffness, pushing force

The biomechanics of force production by the upper limb has been the object of several studies. Dempster (1958) reported investigations as far back as 1924. The constant interest from the community is not surprising because force production (often reduced to the action of pulling or pushing) is a physical action present in most of our daily activities as well as in the workplace environment. To properly fit tools, environments, and workplaces to humans' motor control capabilities, one needs to know what factors limit pushing and pulling and to have a better understanding of the mechanics of force exertion.

Using a free-body diagram in a static analysis, Dempster (1958) observed that while individuals are standing, their maximum pulling force magnitude is limited by their ability to displace their center of mass (CM) horizontally away from the center of pressure (CP) at the foot. That finding, of course, is valid only when individuals perform constant pulling force tasks. Others have shown that standing individuals can also take advantage of the angular momentum H of their body to produce force impulses (Michaels & Lee, 1996; Wing, Flanagan, & Richardson, 1997). That motor control strategy can be easily captured by a simple inverted pendulum model for the standing subject (Pai & Patton, 1997). By providing angular momentum to their body prior to producing a pulling or pushing force, individuals can greatly increase their pulling or pushing force capability, because momentum H will compensate for the opposing angular momentum subsequently produced by the impulse hand interaction force. The allowable peak force is physically limited, in part because of the constraint that individuals must maintain stability following force exertion (Pai & Patton, 1997). However, the momentum strategy is effective only when brief transient forces are desired. For constant pushing force exertion, Grieve (1983) showed that the CM motion is not the only strategy that individuals can use to modulate force magnitude. Other strategies exist, and those will be described in more detail in the next section.

In many studies, researchers have investigated different biomechanical factors that may influence the pushing or pulling force capabilities of a human subject. Results have shown that the individual's weight and height (Chaffin, Andres, & Garg, 1983), floor friction coefficient (Kroemer, Kroemer, & Kroemer-Elbert, 1994), pushing height (Chaffin, Andres, & Garg, 1983; Kumar, 1995), body posture (Daams, 1993), pushing frequency and duration (Snook & Ciriello, 1991), and foot placement (Warwick, Novak, &

Correspondence address: Denis Rancourt, Department of Mechanical Engineering, Laval University, Pavillon Pouliot, Room 1504, Sainte-Foy Québec, G1K 7P4, Canada. E-mail address: boloria@gmc.ulaval.ca

Schultz, 1980) all influence the maximum force produced. Force magnitude may also be limited by the instability induced by the force itself under certain conditions, such as pushing on a pivoting stick. In fact, Bober, Kornecki, Lehr, and Zawadzki (1982) reported a decrease of up to 26% in pushing force magnitude in such conditions. Even more significant diminutions, of over 50%, were observed in a recent study by Roy (1999).

To our knowledge, hand force exertion studies have so far been limited to the context of impulsive and constant pulling or pushing force conditions. Our aim in the present study was to extend the biomechanical analysis of hand pushing force by considering the problem of dynamically controlling its magnitude. That issue is important in hand tool operations such as drilling, sanding, and grinding, because tool operators often have to change the hand–tool interaction force to properly perform the task. The analysis presented here is based on a simple dynamic human motor control model. The advantage of such a model is that it is valid for both static and dynamic force exertion situations and it incorporates limb mechanical impedance as an important biomechanical factor in the physics of force exertion.

In this article, we first present a static analysis of the pushing force of a standing individual to explain different strategies that can be used to modulate pushing force magnitude. Although a similar analysis was reported in an earlier article (Grieve, 1983), the static analysis is an essential part in the development of a dynamic model of pushing. In particular, the static analysis provides estimates on how much each motor control strategy might be effective at varying force magnitude.

One well-known strategy that a standing individual can use to modulate pushing force is to displace the CM of the body away from the CP. If the hand is not making contact with a stable environment, the individual must maintain the CM within the base of support (BOS) at steady state to ensure static postural stability (e.g., Pai & Patton, 1997). When the BOS is restricted to the foot surface, the physical range of pushing force variations is therefore limited if the CP must remain within the BOS; that limitation, however, is usually not required. Larger variations in pushing force are feasible when an individual moves one leg forward so that the size of the BOS is increased. In the present article, the resulting posture is called a *feet-apart posture* (Figure 1, left) as opposed to a *feet-together* or *parallel-feet posture* (cf. Figure 1, right). We will show that such a posture is convenient not only to increase the range of allowable force variations but also for proper control of pushing force. Indeed, that stance prevents the occurrence of unwanted dynamics when pushing force magnitude must be changed. That nonintuitive physical phenomenon is well represented by the dynamic model developed in this article. The model is based on the fact that the upper limb has a nonzero output mechanical impedance (e.g., Bizzi, Accornero, Chapple, & Hogan, 1982; Feldman, 1966), which is critical for the stability of the limb and body. The model clearly demonstrates the influence of body posture, in particular foot placement, on the ability of an individual to dynamically control pushing force. In addition, it demonstrates the influence of limb stiffness in the pushing force task, an issue that was introduced in an earlier article (Michaels & Lee, 1996).

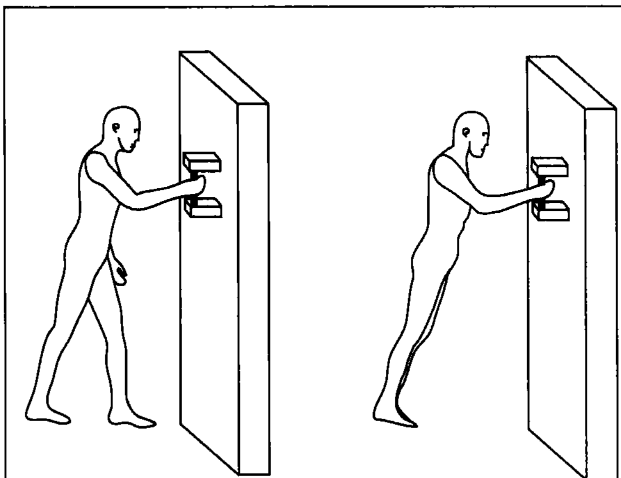

FIGURE 1. Human pushing on a fixed handle in (**left**) feet-apart posture and (**right**) parallel-feet posture.

Theoretical Analysis

Different Strategies for Producing Pushing Force

One can best achieve a description of different strategies for exerting or controlling a pushing force for a standing individual by using a static analysis of a person who pushes on a fixed object, such as a handle fixed on a wall (see Figure 1). In our analysis, we considered at least five different ways to produce a pushing force. In this section, we describe four of the strategies by modeling a standing individual as a simple inverted pendulum (see Figure 2), and we discuss the fifth strategy in the next section.

Static equilibrium of the pendulum in the sagittal plane leads to the following moment balance equation about the contact point, that is, the CP:

$$F_x L_1 \sin\theta - mgL_{CM}\cos\theta - F_y L_1 \cos\theta - \tau = 0, \quad (1)$$

where F_x is the horizontal component of the interactive force between the hand and the wall; F_y is its vertical component; m is the individual's body mass; g is the gravitational acceleration; L_{CM} is the distance between the CM and the CP; L_1 is the shoulder height for a straight-standing subject; θ is the sway angle of the pendulum about the horizontal, that is, the body tilt angle, where 90° is upright; and τ is the moment interaction between the hand and the wall. If we consider the horizontal component of the interactive force, F_x, then

$$F_{push} = F_x = mg\frac{L_{CM}}{L_1}ctg\theta + \frac{\tau}{L_1\sin\theta}. \quad (2)$$

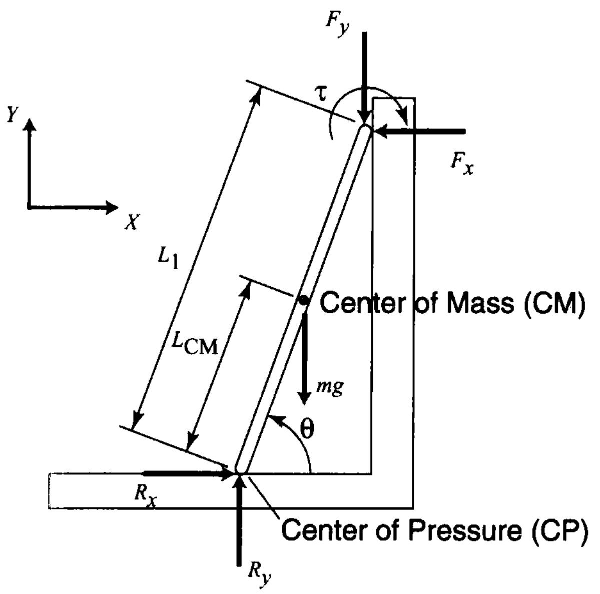

FIGURE 2. Inverted pendulum model of an individual pushing, point contact model. See "Theoretical Analysis" for definitions.

Equation 2 indicates that F_x can be produced or controlled either by the action of gravity, the action of a vertical force F_y or a moment τ. Hence, one can control pushing force by modifying either L_{CM}, θ, F_y, or τ. Those observations were previously described by Grieve (1983) in the context of slipping caused by manual exertion.

One can increase L_{CM}, for example, by raising one leg along the body (i.e., flexing the hip and the knee to raise the leg upward) or by moving one lower limb forward without making contact with the ground. The body tilt angle θ is mainly determined by the position of the contact point (i.e., the CP), the upper limb configuration, and the height of the hand, three variables that can be chosen within a certain range by the individual. Once the hand location, feet pattern, and location are defined, one can still modulate pushing force by changing the upper limb configuration; that strategy, which is commonly described as "pushing with the body," makes the body tilt forward or backward, thereby modifying pushing force magnitude. One can also modify pushing force magnitude by changing the vertical force F_y exerted on the wall. We speculate that that strategy may be associated with what most people perceive as pushing with the arm. We base that hypothesis on two observations: First, the pushing with the arm strategy does not require any modification of body tilt angle. Second, because of the large moment arm of vertical force F_y relative to the shoulder, upper limb muscles become significantly loaded, thereby associating pushing force with upper limb muscle activation. Such a strategy for controlling pushing force is not always desirable; for example, in horizontal drilling, an individual who uses such a strategy would exert side loads on the drill that might break the bit. Finally, one can change pushing force magnitude by modulating the magnitude of the moment τ produced by the hand on the wall. That strategy is often not practical in tool usage because the interface of the tool with the environment cannot transmit moments in the appropriate directions.

Use of CP to Modulate Pushing Force

The inverted pendulum model standing on a fixed contact point cannot represent one important strategy for modulating pushing force: that of moving the CP within the BOS. Because the contact of the foot with the ground is actually not a point but a finite surface, individuals have the ability to modify the CP location without any appreciable change in body configuration and CM location, as is illustrated in Figure 3. For instance, the body can tilt forward so that the CM is over the anterior portion of the BOS. If an individual locates the CP in that region, the pushing force may become negligible. If the CM is posterior to the CP, then pushing force can even become negative; that is, it becomes a pulling force. The range of pushing force variations that can be achieved with that strategy is directly related to the BOS size. One can significantly increase that range by choosing a feet-apart posture as opposed to a parallel-feet posture, as shown in Figure 1.

How Is Pushing Force Actually Produced?

As described in previous sections, there are at least five different strategies for producing a constant pushing force for a standing individual: (a) raising the center of mass along the body, (b) using a vertical hand force, (c) using a hand moment, (d) tilting the body as a whole, and (e) using CP motion over the BOS in a parallel-feet or feet-apart pos-

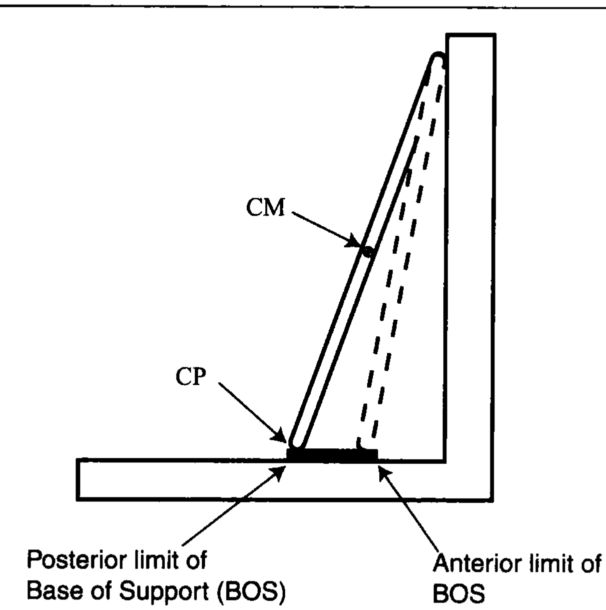

FIGURE 3. Practical range of body tilt angle configuration when moving the center of pressure (CP) location from the anterior limit of the base of support (BOS) to its posterior limit. CM = center of mass.

ture. A priori, it is not possible to determine which strategy is used under what conditions. Some of the strategies may be appropriate for producing small pushing forces or small magnitude changes for increased accuracy in force control. Some may not be possible because the contact environment cannot transmit the necessary forces or moments. The momentum strategy mentioned earlier may be appropriate when large forces are required over short periods of time (e.g., opening a door or hitting an object) but is inappropriate when producing steady forces, which are often necessary when operating hand power tools. There is therefore a need to determine the effectiveness of strategies for producing constant forces.

By using the following anthropometric values obtained from Kroemer et al. (1994, pp. 30 and 80) and Chaffin and Andersson (1991, p. 80) for an average-size man—mass m = 78 Kg, height L = 176 cm, shoulder height $L_1 = 0.818 \times 176$ cm = 144 cm, center of mass height $L_{CM} = 0.588 \times 176$ cm = 104 cm, and body tilt angle $\theta = 80°$—we computed theoretical estimates of the range of pushing force magnitudes that can be achieved by each strategy. Pushing force ranges for all five strategies are listed in Table 1.

As mentioned earlier, one can change L_{CM} by raising either the free upper limb or the lower limb upward along the body (i.e., flexing the hip and the knee so that the leg is raised upward) or anteriorly. The latter type of movement is discussed later in this section. As a limit case, let us assume

TABLE 1
Theoretical Estimates of Pushing Force Maximum Range for All Pushing Strategies

Pushing strategy	Maximum pushing range (N)
For given body tilt angles (90° = upright)	
80° body tilt angle	
Hand moment (τ strategy)	7
Raising lower limb (L_{CM} strategy)	6
Vertical force (F_y strategy)	19
70° body tilt angle	
Hand moment (τ strategy)	7.4
Raising lower limb (L_{CM} strategy)	11
Vertical force (F_y strategy)	37
Over practical values of body tilt angles	
Body tilt angle strategy	10 N/deg
CP motion strategy	
Parallel-feet posture[a]	77[b]
Feet-apart posture[c]	655[d]
Momentum strategy	1,100[e]

Note. Data estimated in the Table are for an average-sized man. [a]The minimum body tilt angle is about 82°. [b]Wing et al. (1997) actually found values on the order of 30 N. [c]The minimum body tilt angle is about 40°. [d]Because of slipping, this value is much lower in practice. [e]Data were obtained from Michaels et al., 1993.

that one of the lower limbs is now concentrated at hip level. The new CM would become located at about L_{CM} = 110 cm, a variation of only 5.5% in the location of the CM. Based on Equation 2, the maximum percentage change in pushing force is therefore limited to 5.5%. When we used the anthropometric values denoted earlier, we found a maximum absolute change of about 6 N in pushing force, (cf. Table 1). Larger changes are obtained for smaller body tilt angles: For a body tilt angle of 70°, the variation in pushing force increases up to 11 N for the same lower limb configuration change.

If variations in pushing force are produced by a change in the vertical force F_y, the possible range of variation is about twice as much. Based on Equation 2, the pushing force is directly proportional to F_y by a factor of $ctg\theta = 0.18$ for θ = 80°. Assuming that an individual can produce a maximum F_y of about 107 N (Rohmert, 1966, cited in Chaffin & Andersson, 1991), one can therefore modulate pushing force by no more than 19 N with such a control strategy (cf. Table 1). For a body tilt angle of 70°, the maximum variation in pushing force increases up to 37 N.

If variations in pushing force are produced by a change in hand moment τ, the possible range of variation is much smaller. For θ = 80°, and assuming that the maximum moment that a hand can produce perpendicular to the sagittal plane is on the order of 10 N-m, Equation 2 shows that one can achieve a maximum variation of only 7 N in the pushing force by using the hand moment strategy (cf. Table 1). Even for a body tilt angle of 70°, the force variation is limited to 7.4 N.

More effective strategies for modulating pushing force can be chosen. For instance, if one chooses the body tilt angle strategy, the variation in pushing force for the anthropometric values indicated earlier is about δF_{push} = 10 N/deg. For a body tilt angle variation of 10° only, pushing force can be modulated by about 100 N (cf. Table 1). However, the maximum force produced with that strategy is limited by the individual's weight, the floor's friction characteristics, and the ability of the individual to maintain the body in a rigid stable configuration.

Finally, one can also modulate pushing force by changing the CP location. In practice, that is equivalent to changing body tilt angle without an actual change in body configuration or in the CM. Let us assume first that the CM is restricted to the BOS surface. For a parallel-feet posture, the BOS size is physically limited to a certain region of the foot length, that is, about 15 cm. Under such conditions, the minimum achievable body tilt angle is about 82°; in that position, the CM is over the most anterior portion of the BOS and the CP is at the most posterior portion of the BOS, as shown in Figure 3. Assuming that Equation 2 is valid in the present case, those values lead to a maximum variation in pushing force of 77 N (cf. Table 1), the minimum being 0 N when the CM is set over the CP location. If the CM exceeds the BOS, pushing force is then achieved in conjunction with the body tilt angle strategy.

One can achieve a larger BOS by moving one foot forward anterior to the CM and even anterior to the shoulder location. In that stance, which is called the *feet-apart posture*, the BOS can be made as long as about 80 cm. When the CM is located at the posterior limit of the BOS, the body tilt angle is at a minimum around 40°. On the basis of Equation 2, therefore, we calculated the maximum range of pushing force as 655 N (cf. Table 1), because the minimum is 0 N when the CM is set over the CP. In practice, the range is much lower because of the physical limitations caused by slipping on the floor or by limited upper limb force exertion capabilities.

In summary, two different strategies seem to be the most effective for producing large variations in pushing force: the body tilt angle strategy and the CP motion strategy in which a feet-apart posture is used. Although by using the parallel-feet posture, one can achieve significant force variations, the maximum force that can be produced in that posture is on the order of 77 N, based on anthropometric values for an average-size man. That amount of force may not always be sufficient in certain interactive tasks. For instance, hand power tool usage may often require larger pushing forces (over 100 N), which one can produce only by using one of the two most effective strategies or by using the CP motion with a parallel-feet posture in conjunction with a vertical force whenever the environment or the upper limb can resist such a force.

From a static analysis viewpoint, the body tilt angle and the CP motion strategies have a similar capacity for producing pushing forces. However, a dynamic analysis of pushing reveals a striking difference between the two pushing strategies. To describe that phenomenon, we developed a dynamic model of a standing subject performing a pushing task.

Dynamic Model of the Pushing Force Task

Our aim in presenting the dynamic model is to describe how a pushing force varies with time when an individual is asked to change the force magnitude by using either the body tilt angle strategy with a parallel-feet posture or a CP motion strategy. We developed a dynamic model for each pushing case. We show herein that each strategy exhibits different force transient dynamics when the pushing force is modified.

Dynamics of the Body Tilt Angle Strategy

In this analysis, we assumed that the individual pushes on a fixed handle, with feet together as shown in Figure 1 (right), producing a pushing force F_0 caused by the action of gravity. For clarity, we also assumed that both τ and F_y remain negligible during the task and that L_{CM} remains practically constant. In the following analysis, the contact surface is modeled as a simple contact point; that is, the CP is constrained to a given location of the foot surface. That constraint is, of course, not exactly realistic, because an individual can modify the CP anywhere on the foot surface while pushing. That particular case is analyzed in the following section. If the individual is asked to decrease or increase pushing force magnitude, he or she is left with one solution, that is, to increase or decrease body tilt angle by extending or retracting the upper limb. One can analyze the overall effect of changing body tilt angle on the dynamic response of the pushing force by modeling the body as a slender rigid bar of length L with its center of mass located at L_{CM} (cf. Figure 4). To decrease the horizontal pushing force from an initial value F_0, to a final value F, one must increase the body tilt angle from an initial value θ_0, to a final value θ. Transiently, that change requires the body to be accelerated toward the upright position. That acceleration, in turn, requires a transient increase in horizontal pushing force to a value greater than F_0, before its subsequent decrease to F. A similar initial reversing behavior also occurs when the horizontal pushing force must be increased.

The details of the force transient depend in part on the mechanical impedance of the upper limb. To represent that phenomenon, we modeled the upper limb as a linear spring of stiffness K_1. This model is extremely simplified because the upper limb mechanical impedance exhibits considerably more complex dynamics that are also highly nonlinear. It is adequate for our present purpose, however. To include dissipation in our model, we assumed a damper of constant b at the ankle joint. Although experimental values of ankle joint damping properties are reportedly about 1 N-m-s/rad (cf. Kearney & Hunter, 1982), one needs a damping value as high as 200 N-m-s/rad to ensure rapid convergence of the pushing force. That finding suggests that other joints and muscles that connect the hand to the foot also contribute to damping during pushing. If damping from those joints had been modeled, in particular those from the upper limb, the ankle damping properties required for convergence would have been much lower.

In our model, it is assumed that pushing force is a consequence of the nonzero mechanical impedance of the upper limb. That approach is consistent with (but does not depend on) the equilibrium-point hypothesis investigated by previous workers (Bizzi et al., 1982; Bizzi, Hogan, Mussa-Ivaldi, & Giszter, 1992; Feldman, 1966; Hogan, 1985; Mussa-Ivaldi, Hogan, & Bizzi, 1985; Shadmehr, Mussa-Ivaldi, & Bizzi, 1993). Different explanations of the neuromuscular origin of this physical behavior have been suggested. In any case, however, because the limb has a demonstrably nonzero mechanical stiffness, there is a point in space where the limb will be in equilibrium. That point is often called the limb *equilibrium point* (Bizzi et al., 1992; Dolan, 1991; Mussa-Ivaldi et al., 1985; Shadmehr et al., 1993). Because sustained external forces can bring the limb to equilibrium at positions other than its equilibrium point, the original equilibrium point is better termed a *virtual position*, that is, a position toward which the hand wants to move. In that context, hand interacting force F and hand position are related by a static relationship in the form of

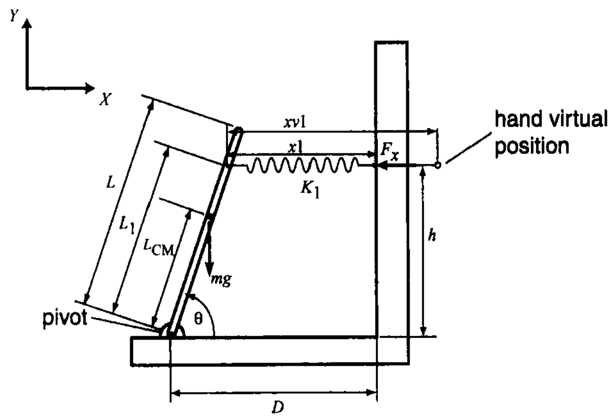

FIGURE 4. Dynamic model of an individual pushing with a body tilt angle strategy with a point-contact condition at the feet. See "Theoretical Analysis" for definitions.

$$F = F(x1, xv1), \tag{3}$$

where $x1$ is the current position of the hand in three-dimensional space and $xv1$ is its current "virtual position," that is, a point in space where the limb would not produce any force (cf. Figure 4). As a first approximation, one can linearize that relationship, which then takes the form

$$F_{\text{push}} = F_x = K_1(xv1 - x1). \tag{4}$$

By changing the hand virtual position $xv1$, an individual can modulate the interacting force while keeping $x1$ constant. Hence, when $xv1 = x1$, no interacting force occurs. According to the model, to generate a pushing force, the pusher must keep $xv1$ greater than $x1$, and, because both values are measured from the shoulder (cf. Figure 4), one solution is to move the virtual position "inside" the wall. The farther the virtual position is moved inside the wall, the larger the interacting force produced. On the basis of this model, one therefore controls pushing force with the hand virtual position.

Using this model of force production by the upper limb, we can find the dynamic response of pushing force following a change in virtual position location by formulating a dynamic equation for an individual whose body rotates about the ankle. Assuming for convenience and without loss of generality that the CM is at the midpoint of the body ($L_{CM} = L/2$), one finds

$$J\ddot{\theta} = F_x L_1 \sin\theta - mg\frac{L}{2}\cos\theta - b\dot{\theta}, \tag{5}$$

where J is the inertia of the body about the ankle and F_x is the interacting force at the hand given by Equation 4. Initially, the individual is at equilibrium. Under that condition,

$$F_{\text{push}} = F_0 = F_{x_0} = K_1(xv1_0 - x1_0). \tag{6}$$

Clearly, an individual can modify or control pushing force magnitude by changing input variable $xv1$. Given that

$$x1 = D - L_1\cos\theta, \tag{7}$$

Equation 5, along with Equation 4, becomes

$$\begin{aligned} J\ddot{\theta} &= K_1(xv1 - x1)L_1\sin\theta - mg\frac{L}{2}\cos\theta - b\dot{\theta} \\ &= G(xv1, \theta, \dot{\theta}). \end{aligned} \tag{8}$$

Because Equation 8 is nonlinear, one can linearize Equation 8 to better explain the dynamic behavior of the system by using common analysis tools of linear system theory . Similarly, Equation 6 can also be linearized so that it provides a transfer function relating small variations $\delta xv1$ of $xv1$ and small variations δF of the pushing force. The detailed development of the linearization procedures used to obtain the transfer function are included in the Appendix, and the result is as follows:

$$\begin{aligned} &\partial F_{\text{push}} \\ &= K_1\left[\frac{Js^2 + bs - K_1L_1^2\cos^2\theta_0 - \dfrac{mgL}{2\sin\theta_0}}{Js^2 + bs + K_1L_1^2\sin^2\theta_0 - \dfrac{mgL}{2\sin\theta_0}}\right]\partial xv1. \end{aligned} \tag{9}$$

Because one of the coefficients in the numerator is always negative, for practical body configurations, the transfer function will contain at least one positive real root, that is, one nonminimum-phase zero. Nonminimum-phase systems are well known in the control theory (cf., Ogata, 1997, p. 486) because they tend to slow down the dynamic response of a system, to cause a reversing behavior at the onset of the response, and they may cause feedback controller instability.

To illustrate how that zero affects an individual's ability to control pushing force, we considered a small change in the virtual position of the hand. To avoid unrealistically rapid transients, we assumed that the virtual position follows a cubic profile lasting 0.5 s (cf. Figure 5, top). Simulations using parameter values that approximate an average-size man are shown in Figure 5, middle. The pushing force dynamic response exhibits a second-order system behavior, as is expected from the transfer function. At the onset of the change in the hand virtual position, however, the pushing force initially increases above its initial value; but it then decreases and quickly converges toward the desired value. In practice, that means that when an individual is asked to decrease pushing force, he or she must first increase the force to make the body rotate backward, thereby reducing the action of gravity; similarly, if the pushing force must be increased, he or she must first reduce it to allow the body to tilt forward, thereby increasing the action of gravity. The existence of such initial reversing behavior is characteristic of linear control systems with nonminimum-phase zeroes in

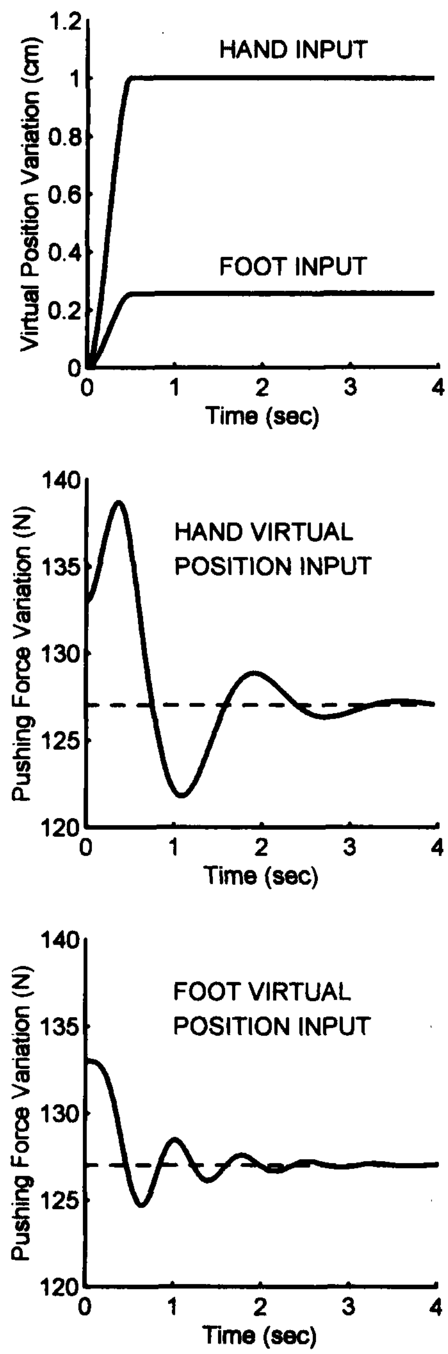

FIGURE 5. Top. Variation in hand or foot virtual position versus time. The top line represents the hand virtual position trajectory profile, whereas the bottom line represents the profile for the foot virtual position trajectory. **Middle.** Variations in pushing force for variations in hand virtual position when a body tilt angle pushing strategy is used. **Bottom.** Variations in pushing force for variations in foot virtual position when a center of pressure (CP) motion pushing strategy is used. These linear simulations were based on the following parameter values, which are those of an average-size man: upper limb stiffness, 1,000 N/m; lower limb stiffness, 19,000 N/m; initial body tilt angle, 75°. We assumed a damper constant b = 200 N-m-s/rad at the ankle. Other parameter values were L_{CM} = 106 cm, L = 176 cm, L_1 = 144 cm, m = 78 kg. See "Theoretical Analysis" for definitions.

the transfer function. Although the system stabilizes to the desired value, the initial reversing behavior may lead to an undesirable response in the pushing force dynamics. One can modulate the zero location at will by changing either G_1, G_2, or G_3 only, because J, the moment of inertia of the individual's body about the ankle, cannot be significantly modified. G_1, G_2, and G_3 can be easily related to the particular physical parameters of the task. The three functions are all determined by body pose and the upper limb impedance selected by the individual to perform the task.

In many situations, that reversing behavior is undesirable. For example, if the task is to drill a through hole, the pushing force should be decreased rapidly as the drill penetrates the work piece. If the pushing force is exerted as described previously, however, any attempt to reduce the force will initially increase it, and that increase may cause excessive penetration of the drill bit. A similar problem may arise in a task as simple as pushing a cart. An abrupt decrease in the cart's rolling resistance (e.g., moving from a carpeted surface to a polished surface) requires a corresponding decrease of pushing force if the cart is not to be accelerated excessively. If the pushing force is exerted as described previously, however, the attempt to decrease the pushing force will initially increase it, exacerbating the problem of unwanted cart acceleration.

Dynamics of the CP Motion Strategy

As discussed previously, in many hand tool applications, an initial transient opposite to the direction of intended change may be undesirable. One can avoid that reversing behavior by using the CP motion strategy, with a feet-apart posture if large forces are required, that is, over 100 N. By moving the CP over the BOS to control pushing force, one can eliminate the nonminimum-phase zero and, consequently, the reversing behavior. The main difference between a parallel-feet and a feet-apart posture while using the CP motion strategy is in the range of achievable pushing forces at which the reversing behavior can be avoided. Referring to Table 1, a parallel-feet posture is limited to pushing forces in the range of 77 N. Forces over 100 N must therefore be achieved in conjunction with other strategies, and in particular the body tilt angle strategy, which is intrinsically a contact point BOS that leads to the reversing behavior.

To illustrate how the reversing behavior can be avoided, we chose a feet-apart posture for the dynamic model by including the lower limb in the dynamic model, as illustrated in Figure 6. This model is more complete because it includes the dynamics of the lower limb in the analysis. In this model, the individual performs the same pushing task by moving one lower limb forward, as shown in Figure 1, left. As a result, the details of the transient also depend on the mechanical impedance of the lower limb, which may be modeled as a linear spring of rigidity K_2, with a virtual position $xv2$ that can be controlled by the individual. On the basis of lower limb stiffness values measured by Greene

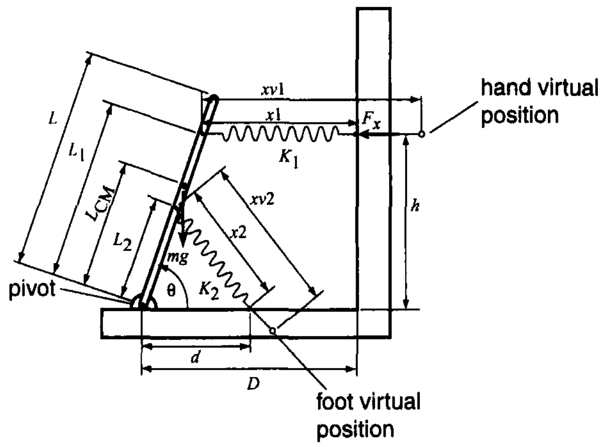

FIGURE 6. Dynamic model of an individual pushing with a feet-apart posture. See "Theoretical Analysis" for definitions.

and McMahon (1979), we chose a stiffness of 19,000 N/m for the rigidity of the spring model. Although the exact value of lower limb stiffness changes the details of the force transient, it does not influence the nonreversing behavior. Therefore, any particular value that maintains a stable body configuration is acceptable to illustrate the phenomenon.

According to this model, by changing or controlling the location of the lower limb virtual position, the individual may change the interacting force between the front foot and the floor and, consequently, may modulate the pushing force produced at the hand. Meanwhile, the hand virtual position may change or remain constant. Such a technique is commonly described as transferring a certain amount of the individual's weight to the front foot or moving the CP forward.

When one modifies pushing force by using input $xv2$ instead of input $xv1$, the reversing behavior observed in the previous model can be avoided: The initial transient of pushing force is in the direction of intended change. To illustrate the issue, we developed the following dynamic model of an individual rotating about the CP of the rear foot:

$$J\ddot{\theta} = F_x L_1 \sin\theta + F_2 r - mg\frac{L}{2}\cos\theta - b\dot{\theta}, \tag{10}$$

where

$$r = \frac{L_2}{x_2} d\sin\theta = \frac{L_2}{\sqrt{L_2^{\,2} + d^2 - 2dL_2\cos\theta}} d\sin\theta, \tag{11}$$

and F_x and F_2 are, respectively, the interacting forces at the hand and the front foot, with

$$\begin{aligned} F_x &= K_1(xv1 - x1), \\ F_2 &= K_2(xv2 - x2). \end{aligned} \tag{12}$$

The pushing force exerted on the wall is still as given by Equation 4. Given that the individual is at equilibrium, Equation 6 is also valid. For convenience, we assumed that the front foot is initially unloaded; that is,

$$F_{2_0} = K_2\left(xv2_0 - x2_0\right) = 0. \tag{13}$$

That equation results in a maximum pushing force magnitude for given foot locations. Using Equations 7, 11, and 12, Equation 10 becomes

$$\begin{aligned} J\ddot{\theta} &= K_1(xv1 - x1)L_1\sin\theta \\ &\quad + K_2(xv2 - x2)\frac{L_2 d\sin\theta}{\sqrt{L_2^{\,2} + d^2 - 2dL_2\cos\theta}} \\ &\quad - mg\frac{L}{2}\cos\theta - b\dot{\theta} \\ &= Q(xv1, xv2, \theta, \dot{\theta}). \end{aligned} \tag{14}$$

On the basis of Equation 14, one can establish a transfer function between small variations $\delta xv1$ of $xv1$, $\delta xv2$ of $xv2$, and corresponding variations δF of the pushing force. The detailed development of the linearization procedures used to obtain the transfer function are included in the Appendix, and the result is as follows:

$$\begin{aligned} \partial F_{\text{push}} &= \partial F_x \\ &= K_1\left[\frac{Js^2 + bs - Q_3 - K_1L_1^2}{Js^2 + bs - Q_3}\right]\partial xv1 \\ &\quad - \frac{K_1K_2L_1L_2d}{xv2_0(Js^2 + bs - Q_3)}\partial xv2, \end{aligned} \tag{15}$$

where

$$\begin{aligned} Q_3 &= -K_1L_1^2\sin^2\theta_0 + \frac{mgL}{2\sin\theta_0} \\ &\quad + K_2L_2d\cos\theta_0\left(\frac{1}{\sqrt{L_2^{\,2} + d^2 - 2dL_2\cos\theta_0}} - 1\right) \\ &\quad - \frac{K_2L_2d\sin^2\theta_0}{\left(L_2^{\,2} + d^2 - 2dL_2\cos\theta_0\right)^{\frac{3}{2}}}. \end{aligned} \tag{16}$$

One can show that the numerator of the first transfer function may still have a negative coefficient for practical ranges of body configurations, whereas the second transfer function is always positive and has no zero. In Equation 15, one can see an important difference in the variation of pushing force resulting from changes in the virtual position of the hand as compared with foot position changes: The transfer function for the foot virtual position does not contain any nonminimum-phase zero. Assuming that the foot virtual position changes follow a cubic profile illustrated in Figure 5, top—similar to the hand virtual position profile, except with a different magnitude—and using the same set of parameters chosen in the previous simulation, we illustrate the resulting dynamic response in Figure 5, bottom. As mentioned earlier, there is indeed no reversing behavior this time. In addition, the time period required to first reach the steady-state value of pushing force is about 0.2 s faster with this strategy than when pushing force is controlled directly by the hand. It also takes about 1 s less to reach a steady-state value. The exact value of those time delays clearly changes with different mechanical parameters of the limbs, but the delays would still remain. One needs a different magnitude in the cubic profile used for the foot virtual position to obtain the same steady-state value of pushing force as in the hand force control simulation.

Discussion

Static Model of the Pushing Force Task

Models more sophisticated than those presented in this article are available for studying pushing (e.g., Andres & Chaffin, 1991; Kerk, Chaffin, Page, & Hughes, 1994). More complete models may produce more accurate results, but they may also make it more difficult to appreciate the basic physical phenomena involved in the pushing task. For instance, using a simple model of pushing, one can easily estimate how different strategies influence the achievable range of pushing force magnitudes. Although the estimates in the present study were for an average-size man, the conclusions from the analysis would be similar for different individuals' sizes. The different pushing strategies reported in this article are also applicable to the pulling case.

Apart from the momentum strategy, a total of five basic strategies were identified in this article: (a) raising the center of mass along the body, (b) using vertical hand force, (c) using hand moment, (d) tilting the body as a whole, and (e) using CP motion over the BOS in a parallel-feet or feet-apart posture. To our knowledge, investigators have provided very little experimental data in the literature to validate the pushing force range for the first three strategies. Despite numerous approximations made in the modeling process, the ranges listed in Table 1 are representative. The first three strategies may be advantageous when an individual accurately controls pushing forces, because the ranges of the forces are limited. The strategies are not adequate, however, when the individual has to generate pushing forces greater than 50 N, for example. For instance, Kroemer et al. (1994, p. 521) reported acceptable pushing forces on the order of 200 N and more for a man exerting sustained forces. In addition, contact environments cannot always resist vertical forces or moments from the hand in certain directions.

Thus, there remain two pushing strategies for producing larger pushing forces: tilting the body or changing the CP location. The body tilt angle strategy has no theoretical maximum pushing force limit. In practice, however, the limit is related either to the maximum shear force that the floor can transmit or to the ability of the individual to maintain the body in a rigid configuration. Data reported in Chaffin and Andersson (1991, p. 320) indicated that actual pushing force limits are in the range of 360 N. Changing the CP location may be more advantageous at the end; simply by changing the CP location relative to the CM, an individual can produce pushing as well as pulling forces for the same body configuration. That strategy also avoids the occurrence of the reversing behavior. When very large transient forces are necessary, an individual can make use of the momentum strategy investigated by previous workers (e.g., Michaels, Lee, & Pai, 1993), who have reported pushing force values as high as 1,100 N. However, that strategy is effective only for producing brief forces with no sustained or steady-state values.

The Importance of Limb Mechanical Impedance in Force-Production Tasks

In the models considered in this article to account for the dynamics of force production, it is recognized that, unlike the "perfect" (zero output impedance) torque or force sources, or both, typically assumed in robotics, real muscles have nonzero output impedance. To account for the nonzero neuromuscular output impedance, we used a model that is consistent with (but does not depend on) the equilibrium-point hypothesis. According to the model, one can modify force magnitude by simply changing the location of the limb virtual position. Although this approach may be unfamiliar, it provides a very simple way of modeling the salient features of the human body in the pushing force task. On the basis of this approach, we have clearly shown in the dynamic analysis that the force dynamic response is highly dependent on limb impedance as well as on body pose. To our knowledge, the importance of limb impedance has not previously been considered. Note that if one uses perfect (zero output impedance) torque or force sources, or both, to generate the forces required for static equilibrium, the pose would be unstable. An analysis of the poles of the transfer function given in Equation 15 indicated that one must maintain upper limb stiffness, for instance, on the order of 800 N/m to prevent unstable poles. That value is in the range of upper limb stiffness levels previously measured (Dolan, 1991; Mussa-Ivaldi et al., 1985; Shadmehr et al., 1993; Won & Hogan, 1995), which suggests that humans could take advantage of the nonzero neuromuscular output impedance to exert pushing forces.

Effect of Foot Placement

By comparing the dynamics of pushing force between the body tilt and the CP motion strategies, we were able to reveal a profound effect of foot placement; a feet-apart posture, in contrast to a parallel-feet posture, enables an individual to properly control pushing force over a larger range of forces when using a CP motion strategy. In fact, if data from Wing et al. (1997) are representative, a parallel-feet posture would not produce more than 30 N of pushing force, assuming that a body tilt angle strategy was not used during testing. Therefore, if larger pushing forces are required, a body tilt angle strategy may be required and a reversing behavior may be observed when changing pushing force. Experimental studies should be undertaken so that investigators can better identify the physical limit of the parallel-feet posture in the pushing force task. The data obtained by Wing et al. (1997) may have been limited by the strength of the fingers in establishing sufficient friction to sustain larger pushing forces.

The fundamental difference between the body tilt and CP motion strategies is whether the individual is standing on a finite BOS area or on a single contact point. With a contact-point situation, changes in force must be preceded by initial changes in the opposite direction; that is, to decrease force, one must first increase it. When the BOS has a finite size, the individual can move the CP on the ground, thereby modulating pushing force magnitude without the occurrence of a reversing behavior. Obviously, a feet-apart posture allows for a larger BOS size and therefore a larger range of pushing forces without the occurrence of a reversing behavior.

A last advantage of using the CP motion strategy over the body tilt angle strategy is that it can produce negative pushing forces, that is, pulling forces, without any change in body configuration. Hand moment or force exertion strategies can also produce pulling forces, although to a much lesser extent.

Conclusions

We have developed a simple static model of the human body in a pushing task that describes various strategies that may be used to modulate steady pushing force magnitude. Five different techniques were identified, and theoretical estimates of how much pushing force each strategy can produce were computed. Although tilting the body forward or backward is an effective way to modulate pushing force magnitude, other strategies may allow more accurate control of small force magnitude variations. A dynamic model of the pushing task showed the significant influence of body pose and limb stiffness on the ability of an individual to dynamically control pushing force. We showed that keeping the feet together in the body tilting technique may induce undesirable dynamic reversals of pushing force when pushing force magnitude must be changed. By assuming a feet-apart posture, one can avoid the problem, because the center of pressure can be moved over a larger base of support. In other words, the best way to control the force at the hand may be by using the foot. Further experimental and theoretical investigations must be undertaken so that a better understanding of the effect of all biomechanical parameters in the performance of the pushing force task can be obtained. However, the data required to understand this apparently simple task are surprisingly complex. At a minimum, the actions of the trunk and lower limb must be considered as well as the actions of the arm and hand.

ACKNOWLEDGMENTS

This work was made possible by the financial help of the Institut de Recherche en Santé et Sécurité au travail of Québec, Canada; by the National Sciences and Engineering Research Council of Canada; and also by U.S. National Institutes of Health Grant AR-40029. Special thanks to Guylaine Fillion for some of the graphics work.

REFERENCES

Andres, R. O., & Chaffin, D. B. (1991). Validation of a biodynamic model of pushing and pulling. *Journal of Biomechanics, 24*(11), 1033–1045.

Bizzi, E., Accornero, N., Chapple, W., & Hogan, N. (1982). Arm trajectory formation in monkeys. *Experimental Brain Research, 46*, 139–143.

Bizzi, E., Hogan, N., Mussa–Ivaldi, F. A., & Giszter, S. (1992). Does the nervous system use equilibrium-point control to guide single and multiple joint movements? *Behavioral and Brain Sciences, 15*, 603–613.

Bober, T., Kornecki, S., Lehr, R. P., Jr., & Zawadzki, J. (1982). Biomechanical analysis of human arm stabilization during force production. *Journal of Biomechanics, 15*(11), 825–830.

Chaffin, D. B., & Andersson, G. B. J. (1991). *Occupational biomechanics* (2nd ed.). Toronto, Ontario: Wiley.

Chaffin, D. B., Andres, R. O., & Garg, A. (1983). Volitional postures during maximal push/pull exertions in the sagittal plane. *Human Factors, 25*(5), 541–550.

Daams, B. (1993). Static force exertion in postures with different degrees of freedom. *Ergonomics, 36*(4), 397–406.

Dempster, W. T. (1958). Analysis of two-handed pulls using free body diagrams. *Journal of Applied Physiology, 13*, 469–480.

Dolan, J. M. (1991). *An investigation of postural and voluntary human arm impedance control.* Unpublished doctoral dissertation, Carnegie Mellon University, Pittsburgh, PA.

Feldman, A. G. (1966). Functional tuning of the nervous system with control of movement or maintenance of steady posture. II. Controllable parameters of the muscle. *Biophysics, 11*, 565–578.

Greene, P. R., & McMahon, T. A. (1979). Reflex stiffness of man's anti-gravity muscles during kneebends while carrying extra weights. *Journal of Biomechanics, 12*, 881–891.

Grieve, D. W. (1983). Slipping due to manual exertion. *Ergonomics, 26*(1), 61–72.

Hogan, N. (1985). The mechanics of multi-joint posture and movement. *Biological Cybernetics, 52*, 315–331.

Kearney, R. E., & Hunter, I. W. (1982). Dynamics of human ankle stiffness: Variation with displacement amplitude. *Journal of Biomechanics, 15*(10), 753–756.

Kerk, C. J., Chaffin, D. B., Page, G. B., & Hughes, R. E. (1994). A comprehensive biomechanical model using strength, stability, and COF constraints to predict hand force exertion capability under sagittally symmetric static conditions. *IIEE Transactions, 26*(3), 57–67.

Kroemer, K., Kroemer, H., & Kroemer-Elbert, K. (1994). *Ergonomics: How to design for ease & efficiency.* Englewood Cliffs, NJ: Prentice Hall.

Kumar, S. (1995). Upper body push-pull strength of normal young adults in sagittal plane at three heights. *International Journal of Industrial Ergonomics, 15*, 427–436.

Michaels, C. F., & Lee, W. A. (1996). The organization of multisegmental pulls made by standing humans: II. Submaximal pulls. *Journal of Motor Behavior, 28*(2), 137–148.

Michaels, C. F., Lee, W. A., & Pai, Y.-C. (1993). The organization of multisegmental pulls made by standing humans: I. Near-maximal pulls. *Journal of Motor Behavior, 25*(2), 107–124.

Mussa-Ivaldi, F. A., Hogan, N., & Bizzi, E. (1985). Neural,

mechanical, and geometric factors subserving arm postures in humans. *Journal of Neuroscience, 5*, 2732–2743.
Ogata, K. (1997). *Modern control engineering* (3rd ed.). Toronto, Ontario: Prentice Hall.
Pai, Y.-C., & Patton, J. (1997). Center of mass velocity-position predictions for balance control. *Journal of Biomechanics, 30*(4), 347–354.
Rohmert, W. (1966). *Maximalkräfte von Männern im Bewegungsraum der Arme und Beine.* [Human maximal force to the upper and lower limb workspace]. Köln, Germany: Westerdeutscher Verlag.
Roy, P.-O. (1999). *Étude des mécanismes de stabilisation d'une tâche de contact par le membre supérieur.* [Analysis of stablization mechanisms in upper limb contact tasks]. Unpublished master's thesis, Université Laval, Québec, Canada.
Shadmehr, R., Mussa-Ivaldi, F. A., & Bizzi, E. (1993). Postural force fields of the human arm and their role in generating multijoint movements. *Journal of Neuroscience, 13*(1), 45–62.
Snook, S., & Ciriello, V. M. (1991) . The design of manual handling tasks: Revised tables of maximum acceptable weights and forces. *Ergonomics, 34*(9), 1197–1213.
Warwick, D., Novak, G., & Schultz, A. (1980). Maximum voluntary strengths of male adults in some lifting, pushing and pulling activities. *Ergonomics, 23*(1), 49–54.
Wing, A. M., Flanagan, J. R., & Richardson, J. (1997). Anticipatory postural adjustments in stance and grip. *Experimental Brain Research, 116*, 122–130.
Won, J., & Hogan, N. (1995). Stability properties of human reaching movements. *Experimental Brain Research, 107*, 125–136.

APPENDIX

Linearization of the Body Tilt Angle Model

The dynamic equation of the body in rotation about the ankle is

$$\begin{aligned} J\ddot{\theta} &= K_1(xv1 - x1)L_1\sin\theta \\ &\quad - mg\frac{L}{2}\cos\theta - b\dot{\theta} \\ &= K_1L_1\sin\theta\, xv1 \;- K_1L_1\sin\theta\; x1 \\ &\quad - mg\frac{L}{2}\cos\theta - b\dot{\theta} \\ &= K_1L_1\sin\theta\, xv1 \;- K_1L_1 D\sin\theta \\ &\quad + K_1{L_1}^2\cos\theta\sin\theta \\ &\quad - mg\frac{L}{2}\cos\theta - b\dot{\theta} \\ &= G(xv1, \theta, \dot{\theta}). \end{aligned} \tag{A.1}$$

Linearizing about the operating point $(xv1_0, \theta_0, \dot{\theta}_0)$ and substituting for θ by using small deviations about the operating point,

$$\begin{aligned} \theta &= \theta_0 + \beta \\ \dot{\theta} &= \dot{\beta} \\ \ddot{\theta} &= \ddot{\beta}. \end{aligned} \tag{A.2}$$

Equation A.1 becomes

$$\begin{aligned} J\ddot{\beta} &= G(xv1_0, \theta_0, \dot{\theta}_0) + \left.\frac{\partial G}{\partial xv1}\right|_0 \partial xv \\ &\quad + \left.\frac{\partial G}{\partial \theta}\right|_0 \partial\theta + \left.\frac{\partial G}{\partial \dot{\theta}}\right|_0 \partial\dot{\theta} \end{aligned} \tag{A.3}$$

with

$$G_1 = \left.\frac{\partial G}{\partial xv1}\right|_0 = K_1L_1\sin\theta_0\ , \tag{A.4}$$

$$\begin{aligned} G_2 &= \left.\frac{\partial G}{\partial \theta}\right|_0 \\ &= K_1L_1\cos\theta_0\;\, xv1_0 - K_1L_1D\cos\theta_0 \\ &\quad + K_1{L_1}^2(1 - 2\sin^2\theta_0) + mg\frac{L}{2}\sin\theta_0 \\ &= -K_1L_1^2\sin^2\theta_0 + \frac{mgL}{2\sin\theta_0}, \end{aligned} \tag{A.5}$$

assuming equilibrium at initial conditions, and

$$G_3 = \left.\frac{\partial G}{\partial \dot{\theta}}\right|_0 = -b. \tag{A.6}$$

One can easily show that at the operating point O,

$$G(xv1_0, \theta_0, \dot{\theta}_0) = 0. \tag{A.7}$$

Hence, (A.3) reduces to

$$J\ddot{\beta} = G_1\delta xv1 + G_2\beta + G_3\dot{\beta}. \tag{A.8}$$

Equation A.8 is linear, and one can easily solve it by using Laplace transformations with all null initial conditions. Equation A.8 becomes

$$\beta(s) = \frac{G_1}{Js^2 - G_3 s - G_2}\,\partial\, xv1(s). \tag{A.9}$$

Similarly, linearization of pushing force magnitude, given by Equation 4, leads to

$$\begin{aligned} \delta F_{\text{push}} &= \delta F_x \\ &= \frac{\delta F_x}{\delta xv1}\delta xv1 + \frac{\delta F_x}{\delta x1}\delta x1 \\ &= K_1(\delta xv1 - \delta x1). \end{aligned} \tag{A.10}$$

For small deviations,

$$\delta x1 \cong \frac{L_1}{\sin\theta_0}\beta, \tag{A.11}$$

and the variation in pushing force magnitude caused by variations in the hand virtual position can be expressed as

$$\begin{aligned} \delta F_{\text{push}} &= \delta F_x \\ &= K_1\left[\frac{Js^2 - G_3 s - G_2 - G_1\dfrac{L_1}{\sin\theta_0}}{Js^2 - G_3 s - G_2}\right]\delta xv1. \end{aligned} \tag{A.12}$$

$$\delta F_{\text{push}} = K_1\left[\frac{Js^2 + bs - G_2 - K_1L_1^2}{Js^2 + bs - G_2}\right]\delta xv1. \tag{A.13}$$

Expanding by using Equations A.4, A.5, and A.6, the transfer function becomes

$$\delta F_{\text{push}} = K_1 \left[\frac{Js^2 + bs - K_1 L_1^2 \cos^2\theta_0 - \dfrac{mgL}{2\sin\theta_0}}{Js^2 + bs + K_1 L_1^2 \sin^2\theta_0 - \dfrac{mgL}{2\sin\theta_0}} \right] \delta xv1. \quad \text{(A.14)}$$

Linearization of the CP Motion Model

The dynamic equation of the body in rotation about the ankle is

$$\begin{aligned} J\ddot{\theta} &= K_1(xv1 - x1)L_1 \sin\theta \\ &\quad + \frac{K_2(xv_2 - x_2)L_2 d \sin\theta}{\sqrt{L_2^2 + d^2 - 2dL_2\cos\theta}} \\ &\quad - mg\frac{L}{2}\cos\theta - b\dot{\theta} \\ &= K_1 L_1 \sin\theta\, xv1 \\ &\quad + \frac{K_2 L_2 d \sin\theta (xv2)}{\sqrt{L_2^2 + d^2 - 2dL_2\cos\theta}} \\ &\quad - K_1 L_1 x1 \sin\theta - K_2 L_2 d \sin\theta \\ &\quad - mg\frac{L}{2}\cos\theta - b\dot{\theta} \\ &= K_1 L_1 \sin\theta (xv1) \\ &\quad + \frac{K_2 L_2 d \sin\theta (xv2)}{\sqrt{L_2^2 + d^2 - 2dL_2\cos\theta}} \\ &\quad - K_1 L_1 D \sin\theta + K_1 L_1^2 \cos\theta \sin\theta \\ &\quad - K_2 L_2 d \sin\theta - mg\frac{L}{2}\cos\theta - b\dot{\theta} \\ &= Q(xv1, xv2, \theta, \dot{\theta}). \end{aligned} \quad \text{(A.15)}$$

Linearizing again about the operating point $(xv1_0, xv2_0, \theta_0, \dot{\theta}_0)$ and using the angle substitution given by Equation A.2, Equation A.15 becomes

$$\begin{aligned} J\ddot{\beta} &= Q(xv1_0, xv2_0, \theta_0, \dot{\theta}_0) \\ &\quad + \left.\frac{\partial Q}{\partial xv1}\right|_0 \partial xv1 + \left.\frac{\partial Q}{\partial xv2}\right|_0 \partial xv_2 \\ &\quad + \left.\frac{\partial Q}{\partial \theta}\right|_0 \partial\theta + \left.\frac{\partial Q}{\partial \dot{\theta}}\right|_0 \partial\dot{\theta}, \end{aligned} \quad \text{(A.16)}$$

with

$$Q_1 = \left.\frac{\partial Q}{\partial xv1}\right|_0 = K_1 L_1 \sin\theta_0 = G_1. \quad \text{(A.17)}$$

$$\begin{aligned} Q_2 &= \left.\frac{\partial Q}{\partial xv2}\right|_0 \\ &= \frac{K_2^2 L_2^2 d^2 \sin^2\theta_0}{xv2_0\sqrt{L_2^2 + d^2 - 2dL_2\cos\theta_0}}. \end{aligned} \quad \text{(A.18)}$$

$$\begin{aligned} Q_3 &= \left.\frac{\partial Q}{\partial \theta}\right|_0 = K_1 L_1 \cos\theta_0 \left(xv1_0 - D\right) \\ &\quad + \frac{K_2 L_2 d \left[\cos\theta_0 - \dfrac{dL_2 \sin^2\theta_0}{L_2^2 + d^2 - 2dL_2\cos\theta_0}\right]}{\sqrt{L_2^2 + d^2 - 2dL_2\cos\theta_0}} \\ &\quad + K_1 L_1^2 (1 - 2\sin^2\theta_0) - K_2 L_2 d \cos\theta_0 \\ &\quad + mg\frac{L}{2}\sin\theta_0 \\ &= G_2 \\ &\quad + K_2 L_2 d \cos\theta_0 \left(\frac{1}{\sqrt{L_2^2 + d^2 - 2dL_2\cos\theta_0}} - 1\right) \\ &\quad - \frac{K_2 L_2 d \sin^2\theta_0}{\left(L_2^2 + d^2 - 2dL_2\cos\theta_0\right)^{\frac{3}{2}}}. \end{aligned} \quad \text{(A 19)}$$

$$Q_4 = \left.\frac{\partial Q}{\partial \dot{\theta}}\right|_0 = -b = G_3. \quad \text{(A.20)}$$

One can easily show that at the operating point O,

$$Q(xv1_0, xv2_0, \theta_0, \dot{\theta}_0) = 0. \quad \text{(A.21)}$$

Hence, Equation A.16 reduces to

$$J\ddot{\beta} = G_1 \delta xv1 + Q_2 \delta xv2 + Q_3\beta + G_3\dot{\beta}. \quad \text{(A.22)}$$

Equation A.22 is linear, and one can easily solve it by using Laplace transformations with all null initial conditions. Equation A.22 then becomes

$$\begin{aligned} \beta(s) &= \frac{G_1}{Js^2 - G_3 s - Q_3}\partial xv1(s) \\ &\quad + \frac{Q_2}{Js^2 - G_3 s - Q_3}\partial xv2(s). \end{aligned} \quad \text{(A.23)}$$

Linearization of pushing force magnitude is given by Equation A.10, and assuming Equation A.11, the variation in pushing force magnitude caused by variations in both virtual positions can be expressed as

$$\begin{aligned} \partial F_{\text{push}} &= \partial F_x \\ &= K_1 \left[\frac{Js^2 + bs - Q_3 - K_1 L_1^2}{Js^2 + bs - Q_3}\right] \partial xv1 \\ &\quad - K_1 \frac{L_1}{\sin\theta_0} \frac{Q_2}{Js^2 + bs - Q_3} \partial xv2. \end{aligned} \quad \text{(A.24)}$$

which becomes the following after expansion of Q_2:

$$\begin{aligned} \partial F_{\text{push}} &= \partial F_x \\ &= K_1 \left[\frac{Js^2 + bs - Q_3 - K_1 L_1^2}{Js^2 + bs - Q_3}\right] \partial xv1 \\ &\quad - K_1 \frac{L_1}{\sin\theta_0} \frac{\left(\dfrac{K_2 L_2 d \sin\theta_0}{xv2_0}\right)}{Js^2 + bs - Q_3} \partial xv2. \end{aligned} \quad \text{(A.25)}$$

Submitted November 2, 1998
Revised June 22, 2000
Second revision November 5, 2000